Kinetics of Protoporphyrinogen Oxidase Inhibition by Diphenyleneiodonium Derivatives[†]

Sylvain Arnould,[‡] Jean-Luc Berthon,[§] Cathy Hubert,[§] Marylène Dias,[§] Christian Cibert,[||] René Mornet,[§] and Jean-Michel Camadro*,[‡]

Laboratoire de Biochimie des Porphyrines, Département de Microbiologie, Institut Jacques-Monod, UMR CNRS 9922-Université Paris 7 Denis-Diderot, 2 Place Jussieu, F-75251 Paris Cedex 05, France, Laboratoire d'Ingénierie Moléculaire et Matériaux Organiques, UMR CNRS 6501-Université d'Angers, Faculté des Sciences, 2 Boulevard Lavoisier, 49045 Angers Cedex, France, and Laboratoire de Physiologie du Développement, Département de Biologie du Développement, Institut Jacques-Monod, UMR CNRS 9922-Université Paris 7 Denis-Diderot, 2 Place Jussieu, F-75251 Paris Cedex 05, France

Received March 11, 1997; Revised Manuscript Received June 4, 1997[⊗]

ABSTRACT: Protoporphyrinogen oxidase, the last enzyme of the common branch of the heme and chlorophyll pathways in plants, is the molecular target of diphenyl ether-type herbicides. These compounds inhibit the enzyme competitively with respect to the tetrapyrrole substrate, protoporphyrinogen IX. We used the flavinic nature of protoporphyrinogen oxidase to investigate the reactivity of the enzyme toward the 2,2′-diphenyleneiodonium cation, a known inhibitor of several flavoproteins. Diphenyleneiodonium inhibited the membrane-bound yeast protoporphyrinogen oxidase competitively with molecular oxygen. The typical slow-binding kinetics suggested that the enzyme with a reduced flavin rapidly combined with the inhibitor to form an initial complex which then slowly isomerized to a modified enzyme-inhibitor complex (K_i = 6.75×10^{-8} M, $K_i^* = 4.1 \times 10^{-9}$ M). This inhibition was strongly pH-dependent and was maximal at pH 8. Substituted diphenyleneiodoniums were synthesized and shown to be even better inhibitors than 2,2′-diphenyleneiodonium: $K_i = 4.4 \times 10^{-8}$ M and $K_i^* = 1.3 \times 10^{-9}$ M for 4-methyl-2,2′-diphenyleneiodonium, $K_i = 2.2 \times 10^{-8}$ M and $K_i^* = 1.1 \times 10^{-9}$ M for 6-methyl-2,2′-diphenyleneiodonium, and $K_i = 6.4 \times 10^{-9}$ M and $K_i^* = 1.2 \times 10^{-12}$ M for 4-nitro-2,2′-diphenyleneiodonium. The 4-nitro-2,2′-diphenyleneiodonium was a quasi irreversible inhibitor ($k_5/k_6 > 5000$). Diphenyleneiodoniums are a new class of protoporphyrinogen oxidase inhibitors that act via a mechanism very different from that of diphenyl ether-type herbicides and appear to be promising tools for studies on the structure−function relationships of this agronomically important enzyme.

Protoporphyrinogen oxidase (EC 1.3.3.4) is the penultimate enzyme in the heme biosynthetic pathway. It catalyzes the oxidative O_2-dependent aromatization of the colorless protoporphyrinogen IX to the highly conjugated protoporphyrin IX (Figure 1). Studies on the structure and function of protoporphyrinogen oxidase were recently stimulated by the discovery of the fact that diphenyl ether-type herbicides are very potent inhibitors of the protoporphyrinogen oxidase activities of yeast, mammal, and plant mitochondria, and plant chloroplasts *in vitro* (*1*, *2*). The phytotoxicity of diphenyl ether-type herbicides is light-dependent and involves intracellular peroxidation promoted by protoporphyrin IX, the heme and chlorophyll precursor, leading to cell damage and lysis (*3*, *4*).

A better understanding of the interactions of diphenyl ether-type herbicides with protoporphyrinogen oxidase requires knowledge of the topological features at the active site of the protein. Radiolabeled acifluorfen (*5*) has been used to demonstrate that several chemically unrelated inhibitors of protoporphyrinogen oxidase share the same binding site on the plant enzyme (*6*). Specifically bound tritiated acifluorfen is also competitively displaced by protoporphyrinogen IX, the substrate of protoporphyrinogen oxidase (*7*). These results are thus in full agreement with kinetic studies showing that diphenyl ethers are competitive inhibitors (with respect to the tetrapyrrole substrate) of plant, mouse, and yeast protoporphyrinogen oxidase (*8*).

An important component of the enzyme catalytic system is the flavin associated with the enzyme, and very little is known of the reactivity of this cofactor. Yeast and mammalian protoporphyrinogen oxidases are FAD-containing enzymes (*9*−*11*). The spectrum of the purified yeast enzyme shows that the flavin is probably in a stable semiquinone form (*12*). The most conserved domain in the primary sequences of yeast, mammalian, plant, and bacterial protoporphyrinogen oxidases is a $\beta\alpha\beta$-ADP binding fold (*13*) near the N terminus of these proteins. This motif is also found in the N-terminal domain of several well-characterized flavoproteins (*e.g.*, monoamine oxidases, and amino-acid oxidases). Although this fact is not formally demonstrated for all protoporphyrinogen oxidases, these enzymes are probably all flavoproteins. This prompted us to further investigate the role of the flavin in catalysis by studying the reactivity of yeast protoporphyrinogen oxidase toward a

[†] This work was supported by grants from the Centre National de la Recherche Scientifique, the Université Paris 7-Denis-Diderot, and the Ministère de l'Education Nationale, de l'Enseignement Supérieur et de la Recherche (Actions Coordonnées Concertées-Sciences du Vivant #5).

* Corresponding author.

[‡] Laboratoire de Biochimie des Porphyrines, Institut Jacques-Monod, UMR CNRS 9922-Université Paris 7 Denis-Diderot.

[§] Laboratoire d'Ingénierie Moléculaire et Matériaux Organiques, UMR CNRS 6501-Université d'Angers.

[||] Laboratoire de Physiologie du Développement, Institut Jacques-Monod, UMR CNRS 9922-Université Paris 7 Denis-Diderot.

[⊗] Abstract published in *Advance ACS Abstracts,* August 1, 1997.

S0006-2960(97)00549-7 CCC: $14.00

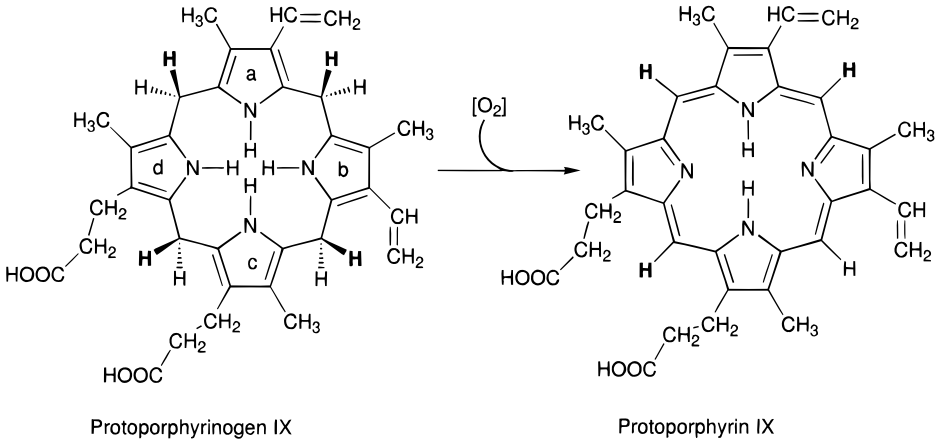

FIGURE 1: Reaction catalyzed by protoporphyrinogen oxidase.

potential inhibitor of flavoproteins, the diphenyleneiodonium cation (DPI).[1] Diphenyleneiodonium and related bis(aryliodonium) species appear to be time-dependent, mechanism-based inhibitors of several flavoproteins such as mitochondrial NADH:ubiquinone oxidoreductase (*14*, *15*), neutrophil NADPH oxidase (*16*, *17*), xanthine oxidase (*16*), nitric oxide synthase (*18*), and cytochrome P450 reductase (*19*). DPIs seem to act on the reduced flavins generated during enzyme turnover, which could act as electron donors to the inhibitor, allowing the generation of phenyl radicals that then covalently modify the flavin or some amino acid side chain important in the catalysis (*20*). In addition to inhibiting flavoproteins, alkynyl and aryl mono- and diiodonium salts are potent inhibitors of pyrroloquinolin quinone-related redox processes (*21*, *22*). The present study shows that yeast membrane-bound protoporphyrinogen oxidase is strongly inhibited by the DPI cation with characteristic slow-binding kinetics. Substitutions on one phenyl ring with methyl or nitro groups produced even more potent slow-binding inhibitors.

EXPERIMENTAL PROCEDURES

Materials. Protoporphyrin IX, disodium salt, was from Serva, FAD from Sigma, and DPI chloride from the Alexis Corp. or synthesized (see below). All inhibitors were dissolved in dimethyl sulfoxide to give 10 mM stock solutions.

General. The protoporphyrinogen oxidase was from mitochondrial membranes of a yeast strain engineered to overproduce this protein. The strain S150-2B*hem14*Δ*::TRP1* transformed with the plasmid pBS19-XS1 (*12*) was grown in 6 L spherical flasks containing 3 L of complete medium (1% yeast extract, 1% bactopeptone, and 2% ethanol as a source of carbon) with constant magnetic stirring and aeration of the growth medium [1 L of air min^{-1} (L of medium)$^{-1}$]. The cells were harvested during the late stationary phase of growth ($A_{600} \approx 30$; 20 g cells wet weight L^{-1}). The membrane fraction enriched in mitochondrial membranes was prepared as described (*23*) and stored at −80 °C. It remained for months without loss of protoporphyrinogen oxidase activity or protein integrity at this temperature when dissolved in 0.1 M potassium phosphate buffer containing 1 mM EDTA, 1 mM dithiothreitol (DTT), and 70 μg mL^{-1} phenylmethanesulfonyl fluoride (PMSF) at 40 mg mL^{-1}.

Chemical Synthesis of Diphenyleneiodonium Derivatives. *DPI Salts*. These salts were prepared according to Collette *et al*. (*24*), with the following modifications. *DPIs Hydrogenosulfate and Chloride.* 2-Iodobiphenyl (108 mg, 0.388 mmol) was dissolved in 0.5 mL of acetic anhydride. A solution of 32% peracetic acid in acetic acid (2 mL) was added dropwise with stirring, and the solution was left at room temperature for 20 h. It was then cooled in ice/water, and sulfuric acid (0.2 mL) was added dropwise; the mixture was kept for a further 20 h at room temperature and then poured into cold water (6 mL). The DPI hydrogenosulfate precipitate was filtered out, triturated with anhydrous diethyl ether, and dried in a dessicator *in vacuo* to give a pale yellow powder (60 mg, 41%) with a mp of 245−250 °C. The filtrate was extracted with toluene (10 mL), and a saturated solution of sodium chloride (4 mL) was added. DPI chloride precipitated and was filtered. It was recrystallized twice from methanol, dried in a dessicator, to give a pale yellow powder (19.1 mg, 16%) with a mp of 281−285 °C [literature mp of 293−298 °C (*25*)]. *DPI Nitrate.* This compound was prepared from DPI hydrogenosulfate, according to Wasylewsky *et al.* (*26*). All DPI salts had identical UV spectra, from water solutions [λ_{max}(nanometers) 264, 256 (sh), 272 (sh), and 290 (sh)].

4-Nitro-DPI Sulfate and Nitrate. These compounds were prepared from DPI nitrate according to Wasylewsky *et al*. (*26*). UV spectra (H_2O): λ_{max} (nanometers) 312 and 313, respectively.

4-Me-DPI Chloride. This compound was prepared in the same way as DPI chloride from 600 mg (2 mmol) of 2-iodo-4-methylbiphenyl (*27*). The expected product was obtained as a gray powder (307 mg, 46%) with a mp of >300 °C. UV spectra (H_2O): λ_{max} (nanometers) 269, 260 (sh), and 278 (sh).

6-Me-DPI Hydrogenosulfate and Chloride. These compounds were prepared as were the corresponding DPI salts, from 700 mg (2.38 mmol) of 2-iodo-2′-methylbiphenyl (*28*). 6-Me-DPI hydrogenosulfate was obtained as a brown powder (300 mg, 32%) with a mp of 267−278 °C and 6-Me-DPI chloride as a brown powder (260 mg, 33%) with a mp of 257−272 °C. UV spectra (H_2O): λ_{max} (nanometers) 266, 257 (sh), 283 (sh), and 296 (sh), for both salts.

[1] Abbreviations: DPI, 2,2′-diphenyleneiodonium; 4-nitro-DPI, 4-nitro-2,2′-diphenyleneiodonium; 4-Me-DPI, 4-methyl-2,2′-diphenyleneiodonium; 6-Me-DPI, 6-methyl-2,2′-diphenyleneiodonium; Tween 80, polyoxyethylenesorbitan monooleate; DTT, dithiothreitol; EDTA, ethylenediaminetetraacetic acid.

^{1}H NMR spectra of DPI, 4-nitro-DPI, 4-Me-DPI, and 6-Me-DPI salts were recorded and found to agree with the corresponding structures.

Enzyme Assay for Kinetic Analysis. Protoporphyrinogen oxidase activity was assayed by measuring the rate of appearance of protoporphyrin fluorescence (*29*). Enzyme assays were carried out at 30 °C. The incubation mixture consisted of 0.1 M potassium phosphate buffer (pH 7.2) saturated with air, containing 2 μM protoporphyrinogen IX, 3 mM palmitic acid (in dimethyl sulfoxide at a final concentration of 0.5% vol/vol), 5 mM DTT, 1 mM EDTA, and 0.3 mg mL^{-1} (final concentration) Tween 80 to ensure a maximal fluorescence signal of protoporphyrin IX. One unit of activity corresponds to the amount of enzyme catalyzing the production of 1 nmol of protoporphyrin IX in 1 h at 30°C. Protoporphyrinogen was prepared by reducing protoporphyrin IX hydrochloride dissolved in KOH/EtOH (0.04 N, 20%) with freshly prepared 3% sodium amalgam (*30*). Stock solutions of protoporphyrinogen [0.1 mM in 0.2 M potassium phosphate buffer (pH 7.2) containing 50 mM ascorbic acid] were kept frozen (−80 °C) under mineral oil and protected from the light for at least 2 weeks. The production of hydrogen peroxide during nonenzymatic oxidation of protoporphyrinogen was measured by a coupled spectrofluorimetric peroxidase assay where a fluorescent dimer of homovanilic acid (nonfluorescent) is formed during the reaction (λ_{em} = 425 nm, λ_{exc} = 315 nm) (*31*). For these experiments, protoporphyrinogen was prepared and stored without ascorbic acid, which is a strong inhibitor of the peroxidase reaction.

When the concentration of dissolved oxygen was varied, the incubation buffer (maintained at 30 °C) was degassed three times under vacuum and then flushed with nitrogen. The desired concentrations of dissolved oxygen were obtained by mixing oxygen-free buffer with various volumes of the same buffer saturated with air. Spectrofluorimetric assays were run in stopped cuvettes to prevent resaturation of buffer with atmospheric oxygen. The final oxygen concentrations were monitored in parallel experiments with a Clark-type oxygen sensitive electrode.

When the effects of pH on protoporphyrinogen oxidase inhibition by DPI were measured, the enzyme was assayed with and without 5 μM DPI in the standard assay medium, while the buffer was varied. We used 0.1 M Pipes for pH 6−6.8, 0.1 M potassium posphate for pH 7.2, and 0.1 M Tris-HCl for pH 7.6−8.6. All buffers were saturated with air at 30 °C.

Data Acquisition in Kinetic Analysis. Progress curves for inhibition of protoporphyrinogen oxidase by DPIs were recorded on an Ifelec 5000 analog recorder coupled to a Jobin Yvon JY3D spectrofluorimeter. Because of the unavoidable uncertainties in the graphical determination of v_s, the data were digitized for fitting the curves to appropriate kinetic equations. This was done by scanning the primary recordings (150 dpi resolution) and processing the scans with a custom written algorithm (Visilog 4.1.1 software, Noesis, France) running on a SiliconGraphics Indigo Entry 4000 workstation. It extracted 600−800 (x,y) unambiguous coordinates from the ebarbed skeleton of each curve, ranked by increasing order on the skeleton. Every point was surrounded by a single pair of neighbors. Experimental data were fitted to appropriate equations with MacCurveFit 1.2.2 software (Kevin Raner Software, Mt. Waverley, Australia). Numerical models of inhibition were developed using the Mathematica 2.2.2 software package from Wolfram Research Inc.

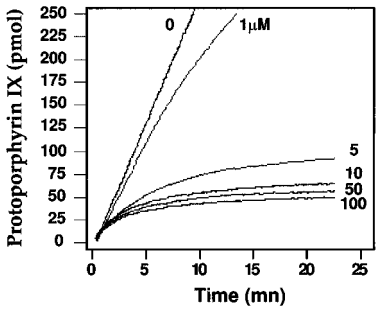

FIGURE 2: Time curve of protoporphyrinogen oxidase activity in the absence (0) and in the presence of 1, 5, 10, 50, and 100 μM DPI. The reaction was initiated by addition of the enzyme (35 units) to the complete incubation medium (1 mL). The increase in protoporphyrin IX fluorescence was recorded (λ_{exc} = 410 nm, λ_{em} = 632 nm).

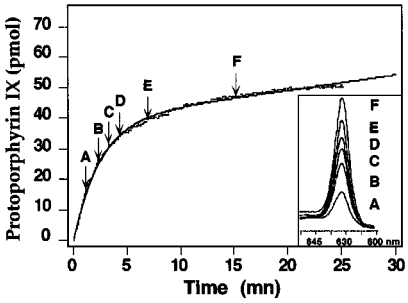

FIGURE 3: Time curve of protoporphyrinogen oxidase activity in the presence of 10 μM DPI overlayed with the best fit to eq 1 ([O_2] = 236 μM, enzyme = 35 units). (Inset) Emission spectra of protoporphyrin IX generated in the assay medium during the reaction. The excitation wavelength is 410 nm. Emission spectra were recorded from 600 to 650 nm.

RESULTS

Kinetics of Protoporphyrinogen Oxidase Inhibition by DPI. The kinetics of protoporphyrinogen oxidase inhibition by DPI were calculated from the curves for protoporphyrinogen oxidase-catalyzed production of protoporphyrin IX in the presence of various concentrations of DPI, with control experiments without inhibitor. The results were independent of the nature of the anion associated with the DPI. All reactions were started by adding the enzyme to the complete incubation medium. The shapes of the time curves (Figure 2) are characteristic of slow-binding inhibition (*32*), where the initial velocity in the presence of inhibitor (v_o) decays to the final steady state velocity (v_s), by a first-order process governed by k_{obs}. The curves were fitted to eq 1

$$[P]_t = v_s t + (v_o - v_s)(1 - e^{-k_{obs}t})/k_{obs} \qquad (1)$$

Figure 3 shows a typical fit of experimental data to eq 1. Spectral analysis of the incubation mixture showed that DPIs did not modify the fluorescence properties of protoporphyrin IX. The finding that the initial velocity in the absence of inhibitor was greater than v_o suggested that the enzyme rapidly combined with DPI to form the initial complex E^{Fl}_{red}–DPI, which then slowly isomerized to E^{Fl}_{red}–DPI (Scheme 1). The equilibrium steps of this process are governed by

Table 1: Kinetic Parameters of Protoporphyrinogen Oxidase Inhibition by DPIs

inhibitor	K_i (M)	k_5 (s^{-1})	k_6 (s^{-1})	K_i* (M)
DPI	$(6.75 \pm 0.15) \times 10^{-8}$	26.0 ± 0.55	1.7 ± 0.03	$(4.1 \pm 0.08) \times 10^{-9}$
4-Me-DPI	$(4.40 \pm 0.25) \times 10^{-8}$	43.5 ± 2.60	1.3 ± 0.08	$(1.3 \pm 0.08) \times 10^{-9}$
6-Me-DPI	$(2.25 \pm 0.15) \times 10^{-8}$	26.7 ± 1.60	1.3 ± 0.08	$(1.1 \pm 0.07) \times 10^{-9}$
4-nitro-DPI	$(6.40 \pm 0.40) \times 10^{-9}$	64.0 ± 2.55	0.012 ± 0.0005	$(1.2 \pm 0.05) \times 10^{-12}$

Scheme 1: Proposed Mechanism of Protoporphyrinogen Oxidase Reaction and Inhibition by DPI[a]

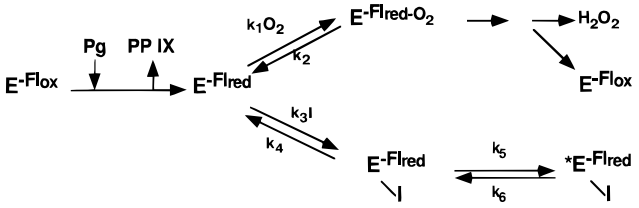

[a] $E^{-Fl_{ox}}$, protoporphyrinogen oxidase with oxidized flavin; $E^{-Fl_{red}}$, protoporphyrinogen oxidase with reduced flavin; Pg, protoporphyrinogen IX; PP IX, protoporphyrin IX.

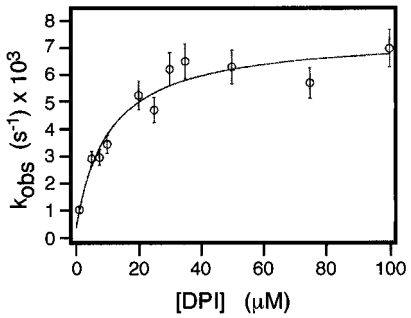

FIGURE 4: : Plot of the apparent rate constant k_{obs} against DPI concentration. The experimental data were fitted to eq 4, where $[O_2] = 236$ μM.

K_i and K_i* which can be calculated from eqs 2 and 3

$$K_i = k_4/k_3 = [E]_{eq}[I]_{eq}/[EI]_{eq} \quad (2)$$

where $[E]_{eq}$, $[I]_{eq}$, and $[EI]_{eq}$ are steady state concentrations of free enzyme, inhibitor and enzyme inhibitor complexes, and

$$K_i^* = K_i k_6/k_5 + k_6 \quad (3)$$

Thus, k_{obs} is related to the mechanistic parameters as described in eq 4, where A is the concentration of dissolved oxygen and K_A the K_m of the enzyme toward oxygen.

$$k_{obs} = k_6 + k_5([I]/K_i)/(1 + [A]/K_A + [I]/K_i) \quad (4)$$

As shown in Figure 4, the secondary plot of k_{obs} against DPI concentration can be fitted to eq 4. We thus determined the main kinetic parameters for the inhibition of protoporphyrinogen oxidase by DPI (Table 1). This approach also allowed us to calculate the K_m of O_2 as 2×10^{-6} M.

The initial velocity (v_o) of the protoporphyrinogen oxidase reaction was measured as a function of DPI concentration at different O_2 concentrations. As shown in Figure 5, the experimental data (Figure 5A) fitted to a numerical model of competitive inhibition (Figure 5B) but not to noncompetitive (Figure 5C) or uncompetitive (Figure 5D) models. The apparent K_m of O_2 [$(2 \pm 0.5) \times 10^{-6}$ M] was independent of the oxygen concentration used in these experiments (from 60×10^{-6} to 236×10^{-6} M).

The inhibition of protoporphyrinogen oxidase by DPI was very sensitive to pH (Figure 6). While the activity of the enzyme in the absence of inhibitor was only sligtly affected by pH (30 units at pH 8.0 vs 35 units at pH 7.2 and 34 units at pH 6.0), the activity in the presence of 5 μM DPI was almost identical to that of controls at pH 6, but strongly inhibited at pH 8. Both v_o and v_s were decreased at these pHs.

The same experimental and formal approaches were used to measure the inhibition of protoporphyrinogen oxidase by 4-Me-, 6-Me-, and 4-nitro-DPI derivatives (Figure 7). All the three compounds showed the same type of slow-binding inhibition of protoporphyrinogen oxidase as DPI (Figure 8). The kinetic parameters of the inhibition were determined as described above (Table 1).

DISCUSSION

We have shown that DPI and its derivatives 4-Me-, 6-Me-, and 4-nitro-DPI are unique inhibitors of protoporphyrinogen oxidase, inhibiting the enzyme via a mechanism different from that of any other inhibitor described to date. The protoporphyrinogen oxidase mechanism of action is still poorly understood. The discovery that diphenyl ether-type herbicides are very powerful inhibitors of eukaryotic protophophyrinogen oxidases stimulated studies on the structure−function relationships and the topology of the active site of the enzyme. Protoporphyrinogen oxidases are flavoproteins, and the occurrence of a flavin at the active site of protoporphyrinogen oxidase may explain some of the catalytic properties of the enzyme. The protoporphyrinogen oxidase reaction is generally described as the removal of six hydrogens from protoporphyrinogen to yield protoporphyrin IX. Ferreira and Dailey (*33*) have indeed reported that the oxidation of 1 mol of protoporphyrinogen IX consumed 3 mol of molecular oxygen and produced 3 mol of hydrogen peroxide. Jones *et al.* (*34*) studied the oxidation of protoporphyrinogen stereospecifically tritiated at the methylene bridges. These authors proposed that three hydrogen atoms from the methylene bridges are removed as hydrides from one side of the protoporphyrinogen molecule, while a fourth one [from the methylene bridge flanking pyrrole rings b and c (Figure 1)] is removed as a proton from the other side. Thus, while the flavin may be involved in hydride removal, another functional group on the protein, possibly a basic amino acid, may be involved in proton removal. This is supported by the molecular dynamics calculations based on QSAR of protoporphyrinogen oxidase inhibitors (*35*, *36*) that point out the potential role of charge transfer and electrostatic interactions in the action of protoporphyrinogen oxidase. In this model, it is implicit that the removal of the hydrides is followed by deprotonation of the nitrogens from the pyrroles to allow the conjugation of the double bonds in the aromatic system of protoporphyrin IX, and the model is consistent with the formation of $3H_2O_2$ during the reaction. However, it is well known that porphyrinogens, including protopor-

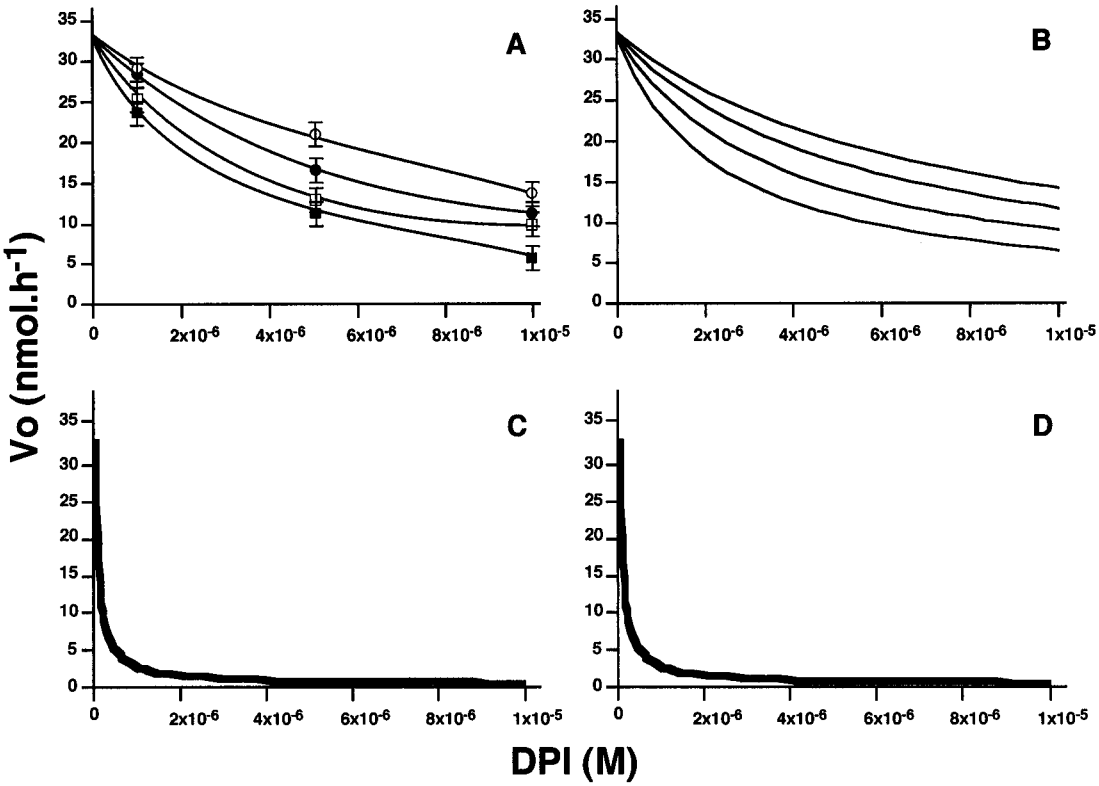

FIGURE 5: (A) Initial velocity (v_o) of protoporphyrinogen oxidase activity mesured in the presence of DPI at different dissolved oxygen concentrations: (○) 236 μM, (●) 178 μM, (□) 118 μM, and (■) 59 μM. The reaction was initiated by addition of the enzyme (35 units) to the complete incubation medium (1 mL). The increase in protoporphyrin IX fluorescence was recorded (λ_{exc} = 410 nm, λ_{em} = 632 nm). (B−D) Numerical models of v_o variations as a function of DPI concentration at different concentrations of dissolved oxygen (from top to bottom, 236, 178, 118, and 59 μM) in a competitive mechanism of inhibition (B), a noncompetitive mechanism of inhibition (C), or an uncompetitive mechanism of inhibition (D).

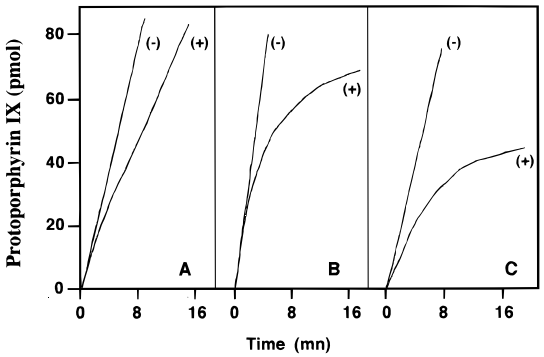

FIGURE 6: : Time curve of protoporphyrinogen oxidase activity in the presence (+) or absence (−) of 5 μM DPI at (A) pH 6.0, (B) pH 7.2, (C) and pH 8.0. The reaction was initiated by addition of the enzyme (35 units) to the complete incubation medium (1 mL). Increase in protoporphyrin IX fluorescence was recorded (λ_{exc}: 410 nm, λ_{em} = 632 nm).

phyrinogen, may be nonenzymatically oxidized to their corresponding porphyrins (*37*). We have shown that the spontaneous oxidation of protoporphyrinogen IX to protoporphyrin IX produces hydrogen peroxide and that the stoichiometry of this reaction is 3 mol of H_2O_2 per mole of protoporphyrinogen. This raises an important question on the mode of action of protoporphyrinogen oxidase. What is the number of redox reactions of the flavin during the catalysis? The mechanism of reaction implies that protoporphyrinogen oxidase must be with an oxidized flavin when the protoporphyrinogen binds to the enzyme and that the reduced flavin generated during protoporphyrin formation must be reoxidized by molecular oxygen. The reaction must thus be of ordered type. But the sequence of the molecular events occurring during the reaction is not clearly established, and two main mechanisms are possible. In the first one, protoporphyrinogen binds to the enzyme with an oxidized flavin and is oxidized by three consecutive steps of reduction−oxidation of the flavin with rotation of the partially oxidized tetrapyrrole intermediates within the active site. A second possible mechanism of protoporphyrinogen oxidase reaction is one where protoporphyrinogen binds to the enzyme with an oxidized flavin and is oxidized through a single reduction−oxidation cycle of the flavin, corresponding to the removal of two hydrogen atoms. Then, the conjugated system obtained might undergo spontaneous and fast oxidation by O_2 with removal of two hydrides from two of the remaining methylene bridges, through a different process, uncatalyzed or involving an unknown cofactor. In both mechanisms, the full aromatization to protoporphyrin IX involves the abstraction of a proton from the last methylene bridge. Whatever the mechanism, the order of the reaction must be one with respect to oxygen, assuming the first step of the reaction is the slowest one. Our experimental data cannot allow us to discriminate between the two mechanisms.

Preincubation of the enzyme with DPI did not modify the mechanism and time course of the inhibition. Inhibition requires incubation of the enzyme with its substrate, protoporphyrinogen IX. This suggests that DPIs react with a reduced enzyme, as already described with other flavoproteins. We have therefore developed a mechanistic model of the interaction of DPIs with protoporphyrinogen oxidase. In this model, DPIs act as competitive inhibitors with respect

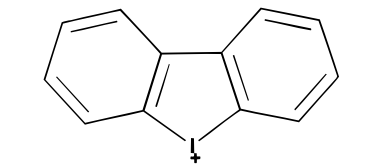

2,2'-diphenyleneiodonium

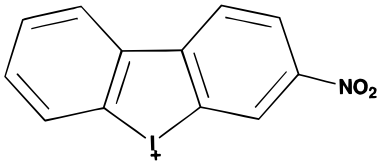

4-nitro-2,2'-diphenyleneiodonium

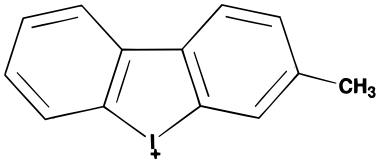

4-methyl-2,2'-diphenyleneiodonium

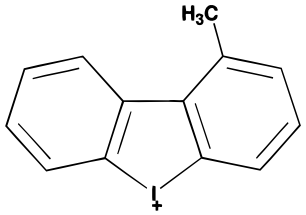

6-methyl-2,2'-diphenyleneiodonium

FIGURE 7: Chemical structures of DPI, 4-nitro-DPI, 4-Me-DPI, and 6-Me-DPI.

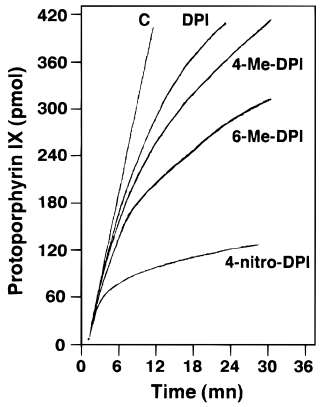

FIGURE 8: Progress curve of protoporphyrinogen oxidase reaction in the absence (C) or presence of 1 μM DPI, or 1 μM 4-Me-DPI, 1 μM 6-Me-DPI, or 1 μM 4-nitro-DPI. The reaction was initiated by addition of the enzyme (35 units) to the complete incubation medium (1 mL). Increase in protoporphyrin IX fluorescence was recorded (λ_{exc} = 410 nm, λ_{em} = 632 nm).

to molecular oxygen during the reoxidation step of the reduced flavin in a simplified overall bi-bi ping-pong mechanism of functioning of the enzyme (Scheme 1). We therefore conducted experiments in which the first substrate of the reaction (protoporphyrinogen) was always saturating, simplifying the rate equation to that for a one-substrate (oxygen) reaction. This model was supported by numerical simulation of the values for v_o and v_s at different concentrations of both inhibitor and oxygen in a bi-bi ping-pong mechanism. While the velocities are strongly dependent on the oxygen concentration in competitive inhibition (Figure 5B), the velocities are almost independent of oxygen concentration in noncompetitive or uncompetitive inhibitions (Figure 5C,D).

There are two main mechanisms of slow binding. In one, the formation of an EI complex is a single slow step; in the other, an EI complex forms rapidly and then undergoes slow and favorable isomerization to an EI* complex. The apparent rate constant (k_{obs}) of the single-step process is a linear function of the inhibitor concentration, while in the second, k_{obs} is a hyperbolic function of this concentration, with an upper limit of $k_5 + k_6$. Our results clearly show (Figure 4) that the inhibition of protoporphyrinogen oxidase by DPIs occurs via the second mechanism. Fitting the experimental values of k_{obs} to eq 4 allowed us to calculate not only K_i and K_i* but also the Michaelis constant for oxygen. The calculated K_m of O_2 (2 μM) is in good agreement with the experimental value of 1.5 $\pm$ 1 μM reported for the yeast protoporphyrinogen oxidase (*9*). The same K_m of O_2 was calculated when protoporphyrinogen oxidase was inhibited by DPI at different oxygen concentrations. Without inhibitor, the large uncertainty of this experimental value was largely due to the difficulty of accurately measuring the low concentrations of dissolved oxygen in the reaction medium down to a fraction of the K_m in a micromolar range. The concentration of dissolved oxygen in potassium phosphate buffer (0.1 M) saturated with air is 236 μM at 30 °C, and mixing strictly degassed buffer with small volumes of buffer saturated with air did not produce accurate concentrations of oxygen below 5−10 μM. Other popular methods of measuring high affinities for molecular oxygen, such as oxygen desorption from oxyhemoglobin, are ineffective in our case because of the strong quenching of the protoporphyrin fluorescence by hemoproteins, which preempts any enzymatic assay. DPI or some of its derivatives may thus be invaluable for estimating the $K_m$of O_2 of other flavoproteins with high affinities for molecular oxygen.

The proposed model for the slow-binding inhibition of yeast protoporphyrinogen oxidase by DPIs assumes that the isomerization step of the enzyme−inhibitor complex is reversible. The exact nature of this isomerization process is still unknown. DPIs probably form a covalent adduct to the reduced flavin of the enzyme, as in cytochrome P450 reductase (*19*), or with free FAD and FMN (*20*) which react with the generated iodobiphenyl radical. How such covalent modification can be reversible within the protein remains to be elucidated. However, preliminary experiments in which the enzyme−inhibitor complexes were separated from free inhibitor by gel filtration and then incubated for several hours with exogenous FAD led to the recovery of a small but significant fraction (10−15%) of the initial activity. This suggests that a covalent complex may be slowly dissociated. This problem will be further assessed using radioiodinated DPI as a probe of the enzyme active site.

The inhibition of protoporphyrinogen oxidase by DPI is very sensitive to pH. The enzyme activity was only slightly inhibited by DPI at low pH (<6.5), but the mode of inhibition (slow binding) remained unchanged. However, at high pH, the enzyme is strongly inhibited by DPI. Control activities measured without inhibitor varied by less than 10% in the same range of pH. The reactivity of reduced flavins toward

different molecular species may vary considerably according to their protonation (*38*) (rate constants vary from 10^4 M^{-1} s^{-1} for the anion radical of the flavin to 10^8 M^{-1} s^{-1} for the neutral radical, in the reaction $FlH^{\bullet} + O_2 \rightarrow Fl_{ox} + O_2^-$). Taking into account these variations, two possible mechanisms may give rise to the higher reactivity of DPI at high pH: greater chemical reactivity of DPI toward anionic reduced flavin, in accordance with the cationic character of DPIs, or decreased competition by oxygen, due to less oxygen activity toward reduced anionic flavin. This second explanation appears to be unlikely, since the reaction rate in the absence of inhibitors does not change much over the pH range used. Spectroscopic studies of the complexes between *purified* enzyme and DPI will be needed to describe these interactions.

Substitutions on the phenyl ring on DPI led to the synthesis of inhibitors of protoporphyrinogen oxidase having the same reactivity toward the enzyme (slow-binding inhibition) on the same order of magnitude as DPI (4-Me- and 6-Me-DPI), or much more efficient (4-nitro-DPI). The inhibition by 4-nitro-DPI is quasi irreversible due to the extremely slow reverse reaction of isomerization ($k_6 = 1.2 \times 10^{-2}$ s^{-1}, $k_5/k_6 = 5340$ compared to $k_6 = 1.7$ s^{-1}, $k_5/k_6 = 15$ with DPI). The strong electron-withdrawing effect of the nitro group in 4-nitro-DPI probably increases the positive charge on the iodine atom, which would favor its electrostatic interaction with an anionic part of the enzyme.

DPIs appear to be extremely valuable tools for studying the structure−function relationships and the topology of protoporphyrinogen oxidase. The slow-binding type of inhibition is of particular interest for developing new specific inhibitors that may act as herbicides because of the extected longer lifetime of the EI* complexes formed with this type of compound (*32*).

ACKNOWLEDGMENT

We thank Prof. Pierre Labbe for his interest and valuable advice. The English text was edited by Dr. Owen Parkes.

REFERENCES

1. Matringe, M., Camadro, J. M., Labbe, P., and Scalla, R. (1989) *Biochem. J. 260*, 231−235.
2. Witkowski, D. A., and Halling, B. P. (1989) *Plant Physiol. 90*, 1239−1242.
3. Sandmann, G., Nicolaus, B., and Böger, P. (1990) *Z. Naturforsch. 45C*, 512−517.
4. Scalla, R., and Matringe, M. (1994) *Rev. Weed Sci. 6*, 103−132.
5. Mornet, R., Gouin, L., Matringe, M., Scalla, R., and Swithenbank, C. (1992) *J. Labelled Compd. Radiopharm. 31*, 175−182.
6. Varsano, R., Matringe, M., Magnin, N., Mornet, R., and Scalla, R. (1990) *FEBS Lett. 272*, 106−108.
7. Matringe, M., Mornet, R., and Scalla, R. (1992) *Eur. J. Biochem. 209*, 861−868.
8. Camadro, J. M., Matringe, M., Scalla, R., and Labbe, P. (1991) *Biochem. J. 277*, 17−21.
9. Camadro, J. M., Thome, F., Brouillet, N., and Labbe, P. (1994) *J. Biol. Chem. 269*, 32085−32091
10. Dailey, T. A., and Dailey, H. A. (1996) *Protein Sci. 5*, 98−105.
11. Dailey, T. A., Dailey, H. A., Meissner, P., and Prasad, A. R. K. (1995) *Arch. Biochem. Biophys. 324*, 379−384.
12. Camadro, J. M., and Labbe, P. (1996) *J. Biol. Chem. 271*, 9120−9128.
13. Wierenga, R. K., Terpstra, P., and Hol, W. G. J. (1986) *J. Mol. Biol. 187*, 101−107.
14. Gatley, S. J., and Sherratt, S. A. (1976) *Biochem. J. 158*, 307−315.
15. Ragan, C. I., and Bloxham, D. P. (1977) *Biochem. J. 163*, 605−615.
16. Doussiere, J., and Vignais, P. V. (1992) *Eur. J. Biochem. 208*, 61−71.
17. O'Donnell, V., Tew, D., Jones, O., and England, P. (1993) *Biochem. J. 290*, 41−49.
18. Stuehr, D. J., Fasehun, O. A., Kwon, N. S., Gross, S. S., Gonzalez, J. A., Levi, R., and Nathan, C. F. (1991) *FASEB J. 5*, 98−103.
19. Tew, D. G. (1993) *Biochemistry 32*, 10209−10215.
20. O'Donnell, V. B., Smith, G. C., and Jones, O. T. (1994) *Mol. Pharmacol. 46*, 778−785.
21. Bishop, A., Paz, M. A., Gallop, P. M., and Karnovsky, M. L. (1994) *Free Radical Biol. Med. 17*, 311−320.
22. Gallop, P. M., Paz, M. A., Flückiger, R., Stang, P. J., Zhdankin, V. V., and Tykwinski, R. R. (1993) *J. Am. Chem. Soc. 115*, 11702−11704.
23. Camadro, J. M., and Labbe, P. (1988) *J. Biol. Chem. 263*, 11675−11682.
24. Collette, J., McGreer, D., Crawford, R., Chubb, F., and Sandin, R. (1956) *J. Am. Chem. Soc. 78*, 3819−3820.
25. Cade, J., and Pilbeam, A. (1964) *J. Chem. Soc.*, 114−121.
26. Wasylewsky, A., Brown, R., and Sandin, R. (1950) *J. Am. Chem. Soc. 72*, 1038−1039.
27. Hellwinkel, D. (1966) *Chem. Ber. 99*, 3642−3659.
28. Hellwinkel, D., Reiff, G., and Nykodym, V. (1977) *Liebigs Ann. Chem.*, 1013−1025.
29. Camadro, J. M., Matringe, M., Scalla, R., and Labbe, P. (1993) in *Target assays for modern herbicides and related phytotoxic compounds* (Böger, P., and Sandmann, G., Eds). pp 29−34, CRC Press/Lewis Publishers.
30. Poulson, R., and Polglase, W. J. (1975) *J. Biol. Chem. 250*, 1269−1274.
31. Guilbault, G., Brignac, P., and Zimmer, M. (1968) *Anal. Chem. 40*, 190−196.
32. Morrison, J. F., and Walsh, C. T. (1988) in *Advances in Enzymology* (Meister, A., Ed.) Vol. 61, pp 201−301, John Wiley & Sons, New York.
33. Ferreira, G. C., and Dailey, H. A. (1988) *Biochem. J. 250*, 597−603.
34. Jones, C., Jordan, P. M., and Akhtar, M. (1984) *J. Chem. Soc., Perkin Trans. 1*, 2625−2633.
35. Akagi, T., and Sakashita, N. (1993) *Z. Naturforsch. 48C*, 345−349.
36. Nandihalli, U., Duke, M., and Duke, S. (1992) *Pestic. Biochem. Physiol. 43*, 193−211.
37. Falk, J. E. (1964) *Porphyrins and metalloporphyrins*, 2nd ed., Elsevier Publishing Co., Amsterdam.
38. Massey, V. (1994) *J. Biol. Chem. 269*, 22459−22462.

BI970549J